

# Molecular Modeling of Substrate Binding in Wild-Type and Mutant *Corynebacteria* 2,5-Diketo-D-gluconate Reductases

Sumit Khurana,<sup>1</sup> Gulsah Sanli,<sup>1</sup> David B. Powers,<sup>2</sup> Stephen Anderson,<sup>3</sup> and Michael Blaber<sup>1\*</sup>

<sup>1</sup>Institute of Molecular Biophysics and Department of Chemistry, Florida State University, Tallahassee, Florida

<sup>2</sup>Department of Anesthesia, University of California, San Francisco, California

<sup>3</sup>Center for Advanced Biotechnology and Medicine and Department of Molecular Biology and Biochemistry, Rutgers University, Piscataway, New Jersey

**ABSTRACT** 2,5-Diketo-D-gluconic acid reductase (2,5-DKGR; E.C. 1.1.1.-) catalyzes the Nicotinamide adenine dinucleotide phosphate (NADPH)-dependent stereo-specific reduction of 2,5-diketo-D-gluconate (2,5-DKG) to 2-keto-L-gulonate (2-KLG), a precursor in the industrial production of vitamin C (L-ascorbate). Microorganisms that naturally ferment D-glucose to 2,5-DKG can be genetically modified to express the gene for 2,5-DKGR, and thus directly produce vitamin C from D-glucose. Two naturally occurring variants of DKGR (DKGR A and DKGR B) have been reported. DKGR B exhibits higher specific activity toward 2,5-DKG than DKGR A; however, DKGR A exhibits a greater selectivity for this substrate and significantly higher thermal stability. Thus, a modified form of DKGR, combining desirable properties from both enzymes, would be of substantial commercial interest. In the present study we use a molecular dynamics-based approach to understand the conformational changes in DKGR A as the active site is mutated to include two active site residue changes that occur in the B form. The results indicate that the enhanced kinetic properties of the B form are due, in part, to residue substitutions in the binding pocket. These substitutions augment interactions with the substrate or alter the alignment with respect to the putative proton donor group. *Proteins* 2000;39:68–75.

© 2000 Wiley-Liss, Inc.

**Key words:** molecular dynamics; molecular modeling; aldo-keto reductase; vitamin C; substrate recognition; 2,5-diketo-D-gluconate; L-ascorbate

## INTRODUCTION

The enzyme 2,5-diketo-D-gluconic acid reductase (2,5-DKGR; EC 1.1.1.-) catalyzes the stereo-specific conversion of 2,5-diketo-D-gluconate (2,5-DKG) to 2-keto-L-gulonate (2-KLG).<sup>1</sup> Two variants of this enzyme from *Corynebacterium* have been identified: DKGR A<sup>1</sup> and DKGR B<sup>2</sup>, also referred to as AKR5C and AKR5D, respectively, in the recently proposed nomenclature for the aldo-keto reductase superfamily.<sup>3</sup> These enzymes are of significant commercial interest because 2-KLG can readily be converted into vitamin C (L-ascorbate).

Vitamin C forms an essential part of the diet of human

beings, and its deficiency causes scurvy, which is characterized by fragile skin, tendons, and blood vessels. Commercially, vitamin C is an important specialty chemical with annual consumption of more than 50,000 tons ( $45 \times 10^6$  kg). At present, the Reichstein and Grussner organic synthesis,<sup>4</sup> developed in the 1930s, is the preferred method for the commercial production of vitamin C. Recently, however, research efforts have been dedicated to developing and improving the industrial synthesis of vitamin C. Most of these have focused on the design of an alternative procedure for commercial production of vitamin C using genetically modified bacteria expressing the gene for 2,5-diketo-D-gluconic acid reductase.<sup>1,2</sup> These genetic manipulations have resulted in bacteria that can directly produce 2-KLG from D-glucose. In principle, this method may have considerable advantage over the currently used Reichstein and Grussner synthesis, which involves numerous chemical steps in addition to a fermentation step.

In order to develop further this new method for vitamin C production, it is necessary to understand the biochemical and biophysical properties of DKGR. This enzyme belongs to the aldo-keto reductase superfamily<sup>3</sup> and shares the common  $(\beta/\alpha)_8$  motif with other members of this family, including human aldose reductase.<sup>5–7</sup> DKGR B is known to be approximately 66 times more catalytically active for substrate (2,5-DKG) as compared to DKGR A (ratio of specificity constants,  $(V_{max}/K_m)_B/(V_{max}/K_m)_A = 66$ ).<sup>8</sup> However, DKGR B exhibits significantly lower thermal stability as compared to DKGR A ( $T_m$  for A variant = 38°C,  $T_m$  for B variant = 32°C).<sup>8</sup>

DKGR A has been the subject of protein engineering efforts to develop a mutant form of DKGR with the thermostability features of DKGR A and the enhanced catalytic features of DKGR B.<sup>8</sup> Based on the related human aldose reductase structure (38% identical), residue positions 22, 49, and 192 were identified as differing between DKGR A and B and potentially localized to the active site region. These residue positions in DKGR A were replaced with the corresponding amino acid residues from

Grant sponsor: Lucille P. Markey Charitable Trust; Grant sponsor: National Institutes of Health; Grant numbers: GM08339, R01AG11525, and R01GM50733.

\*Correspondence to: Michael Blaber, Institute of Molecular Biophysics and Department of Chemistry, Florida State University, Tallahassee, FL 32306-3015. E-mail: blaber@sb.fsu.edu

Received 9 August 1999; Accepted 2 November 1999

DKGR B. The mutations included Phe22Tyr, Gln192Arg, Ile49Asn, and the double mutant Phe22Tyr/Gln192Arg. Although the Ile49Asn mutant could not be isolated (presumably owing to thermal instability), kinetic analyses confirmed that residue positions 22 and 192 can influence catalysis. Substitution to a Tyr residue at position 22 in DKGR A increased  $k_{cat}$  and decreased  $K_m$  constants toward 2,5-DKG, and substitution to an Arg residue at position 192 in DKGR A increased  $k_{cat}$ , with little effect upon  $K_m$ .<sup>8</sup> The double mutant, Tyr22/Arg192, exhibited kinetic properties essentially identical with wild-type DKGR A, indicating that the effects observed in the point mutations were nonadditive.

In the present study we have used a molecular dynamics (MD) conformational search to elucidate the structural determinants of substrate binding in wild-type DKGR A and for the Phe22Tyr and Gln192Arg single and double mutants of DKGR A. A high-resolution crystal structure of 2,5-DKG A indicates that position 49 does not actually constitute part of the binding pocket and is approximately 7 Å away. Subsequently, this mutation was not included in our modeling study. The complexes of wild-type DKGR A, Phe22Tyr, Gln192Arg, and Phe22Tyr/Gln192Arg mutant enzymes with the 2,5-DKG substrate were generated and subjected to 80 ps of MD simulations at 300°K. These structures had, as their starting point, a 2.1 Å X-ray crystal structure of DKGR A/NADPH complex.<sup>5</sup> The simulation yielded a total of 80 structures (sampled after every ps) for each of the complexes which were analyzed for structural determinants of substrate recognition and catalysis. The results of this analysis indicate that Tyr and Arg residues at positions 22 and 192, respectively, directly interact with the substrate C1 carboxylate group. In the case of residue Arg192 this interaction can influence the alignment of the substrate within the binding pocket. Furthermore, the substrate binding pocket of DKGR A appears to be significantly larger than the 2,5-DKG substrate, suggesting that this enzyme may not be optimized for this substrate.

## MATERIALS AND METHODS

### Energy Minimization and Molecular Dynamics

All energy minimization and MD calculations were performed using *DISCOVER* version 3.1 installed with *InsightII* interface (Biosym Technologies, San Diego, CA) as implemented on an SGI *INDY R5000* workstation (Silicon Graphics, USA). The coordinates from the 2.1 Å crystal structure of DKGR A complexed with NADPH were used as a starting model.<sup>5</sup> Hydrogen atoms were added, and amino acid functional groups were ionized corresponding to pH 7.0. The resulting overall charge was neutralized by adding Na<sup>+</sup> counter-ions. All crystallographic water molecules were retained. The NADPH co-factor was modeled in reduced form (as present in the crystal structure) with two hydrogen atoms attached to the C4 atom of the nicotinamide ring. Atomic partial charges and potentials for amino acids and NADPH co-factor were taken from the consistent valence force field (CVFF) as implemented in the *InsightII* package.<sup>9</sup> This approach has been success-

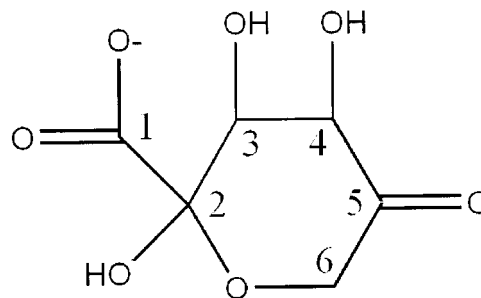


Fig. 1. Structure and nomenclature of the 5-keto form of 2,5-diketo-D-gluconate substrate used in this study.

fully used to model the interaction of lactate dehydrogenase with three substrates.<sup>10</sup>

Coordinates for the 2,5-DKG substrate were generated from the published solution structure.<sup>11</sup> The major structural form of 2,5-DKG in aqueous solution, as determined by <sup>13</sup>C NMR, is the *gem*-diol hydrate at the C5 of the pyranose tautomer with minimal *keto* component.<sup>11,12</sup> However, there is evidence that the enzyme recognizes and stabilizes the *keto*- instead of the *gem*-diol form of the substrate.<sup>13</sup> This is also supported by the crystal structures of substrate complexes of other enzymes belonging to this family, which reveal that these enzymes recognize the *keto* form of the substrate.<sup>14</sup> Therefore, the <sup>13</sup>C NMR structure was modified to have a *keto* group at C5 position of the substrate (Fig. 1). The resulting substrate was subsequently energy minimized and docked into the active site of the wild-type and mutant DKGR enzymes using the docking module of *InsightII*. Two water molecules (solvent 332 and 381, Fig. 2A and B) that are present within the active site of DKGR A in the X-ray structure, and were predicted to be displaced by polar atoms of the bound substrate,<sup>5</sup> were deleted.

A continuous real-time energy calculation was used to manually position the substrate in the active site of DKGR A and the various mutants. In this procedure, the substrate's C5-carbonyl oxygen was positioned within hydrogen bonding distance of the hydroxyl (O<sub>η</sub>H) group of Tyr50, which is generally accepted to be the proton donor for this enzymatic reaction. Furthermore, the substrate's C5-carbonyl carbon atom was kept within 3.0 Å to the 4-*pro-R* hydrogen of the nicotinamide ring of the co-factor in order to facilitate the hydride ion (H<sup>-</sup>) transfer. The starting conformation was selected as the lowest energy conformation obtained by docking the substrate within the active site of each mutant.

The enzyme-substrate complexes were hydrated using a 5.0 Å layer of water molecules around the complexes. In order to limit the necessary computation time to a reasonable time frame, only atoms within a 15 Å radius centered at the Tyr50 O<sub>η</sub> atom were allowed to move. All other atoms were constrained to their relative positions as determined from the high-resolution X-ray crystal structure. A 13.0 Å cutoff for the calculation of non-bonded interactions and a dielectric constant of 1.0 was used throughout the energy minimization and molecular dynam-

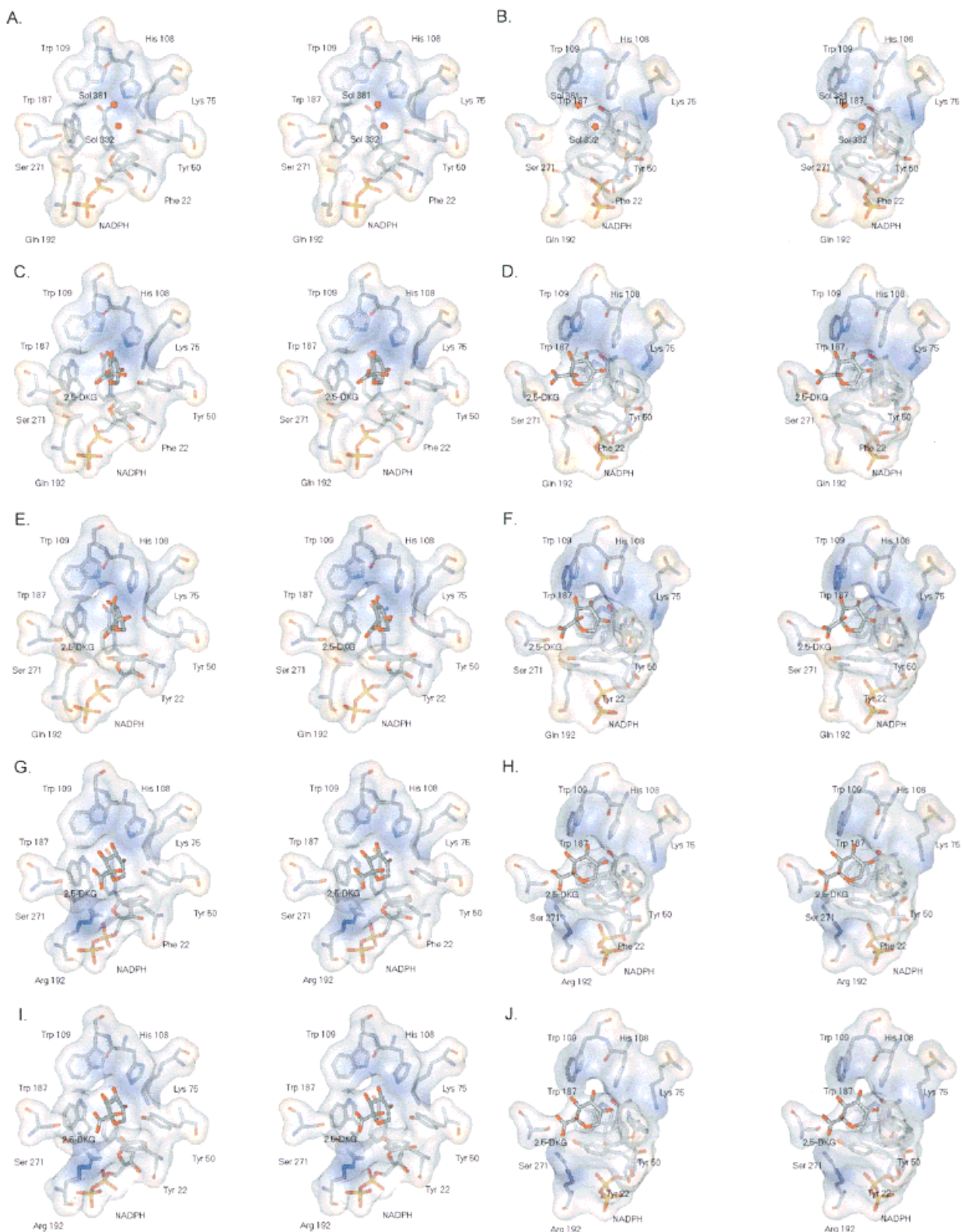


**Fig. 2. A and B:** Stereo diagram of wild-type DKGR A<sup>5</sup> showing residues that define the substrate binding pocket (Phe 22, Tyr 50, Lys 75, His 108, Trp 109, Trp 187, Gln 192, and Ser 271). Also shown are the atoms of the reduced NADPH co-factor within this region as well as two solvent molecules (sol 332 and sol 381) that occupy the pocket as determined from the X-ray crystal structure. The depth of the substrate binding pocket is illustrated in B, which is an approximately 90° rotation of A about the vertical axis. The solvent accessible surface area is shown and is colored to represent the electrostatic potential (blue is positive, red is negative). **C and D:** Wild-type DKGR A active site pocket with bound

2,5-DKG substrate. The structure represents the average of an 80-ps molecular dynamics simulation, sampled every picosecond. **E and F:** Active site pocket of the Phe22Tyr mutation of DKGR A with bound 2,5-DKG substrate (average of an 80-ps molecular dynamics simulation, sampled every picosecond). **G and H:** Active site pocket of the Gln192Arg mutation of DKGR A with bound 2,5-DKG substrate (average of an 80-ps molecular dynamics simulation, sampled every picosecond). **I and J:** Active site pocket of the Phe22Tyr/Gln192Arg double mutation of DKGR A with bound 2,5-DKG substrate (average of an 80-ps molecular dynamics simulation, sampled every picosecond).

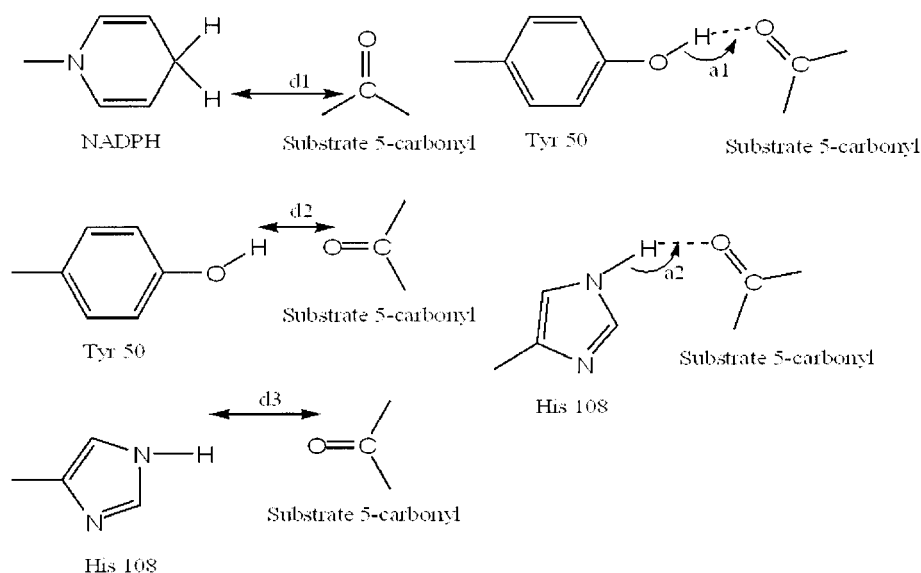


Fig. 3. Sets of conformational parameters analyzed for wild-type DKGR A, and point mutants Phe22Tyr and Gln192Arg with bound 2,5-DKG substrate. Parameters d1, d2, and d3 represent distances, and a1 and a2 represent angles.

**TABLE I. Side Chain Fluctuations ( $\text{\AA}$ )<sup>†</sup> in the Active Site of 2,5-DKGR A and Various Mutants Upon Binding of 2,5-DKG Substrate**

Enzyme	Phe/Tyr22	Tyr50	His108	Trp109	Gln/Arg192	NR <sup>a</sup>
DKGR A	0.12	0.15	0.13	0.21	0.23	0.24
F22Y	0.19	0.16	0.13	0.14	0.33	0.37
Q192R	0.50	0.51	0.65	0.61	0.67	0.35
F22Y/Q192R	0.90	0.71	0.76	0.75	0.87	0.57

<sup>†</sup>Average root mean square deviation between energy-minimized X-ray structure and the 80 simulated structures for each mutant.

<sup>a</sup>Nicotinamide ring.

ics calculations. Initially, the structures were minimized for 200 cycles of steepest descent by fixing all the protein and substrate atoms and allowing the water molecules to move. This was followed by 200 cycles each of steepest descent and conjugate gradient minimization. During this minimization, all atoms were tethered with a force of 100 kcal/mol, which permitted the relaxation of bad van der Waals interactions. Subsequently, this step was repeated without any restraint until an average derivative of less than 0.05 kcal/mol/ $\text{\AA}$  was reached. The resulting structure was used as a starting point for sampling conformational space using molecular dynamics. Each energy-minimized complex was equilibrated at 300°K for 10 ps using the Verlet algorithm.<sup>15</sup> Following this, an 80-ps simulation was carried out at 300°C, and structures were sampled at a regular interval of 1 ps. The sampled structures were, subsequently, energy minimized using conjugate gradient minimization prior to conformational analysis.

### Calculation of Interaction Enthalpies and Solvation Energies

The van der Waals and electrostatic component of interaction energies between the substrate and enzyme were calculated using the docking module of *InsightII*. The interaction enthalpies so obtained were corrected for solvation effects by calculating the electrostatic component of the free energy of solvation for enzyme, substrate, and

enzyme–substrate complex for each of the mutants using the Delphi module of *InsightII*. All water molecules were removed before performing these calculations. The solvation energies for enzyme, substrate, and enzyme–substrate complex were in each case obtained as the difference of calculations between a solvent dielectric of  $\epsilon = 78.6$  and  $\epsilon = 1.0$ . All calculations were performed with a relative permittivity of 2.0 inside the protein to account for electronic polarizability, and ionic strength was fixed at 0 mol/dm<sup>3</sup>. After calculation of the solvation energies, interaction enthalpies between enzyme and substrate were corrected for solvation effects by subtracting the solvation energies of enzyme and substrate from that of enzyme–substrate complex.<sup>16,17</sup>

## RESULTS

### Substrate Binding in Wild-Type DKGR A

A stereo-view of the average structure over an 80 ps MD simulation for the wild-type enzyme–substrate complex is shown in Figure 2 (C and D). The root mean square deviation of the active site residues averaged over the 80-ps MD simulation is less than 1.0  $\text{\AA}$  from the energy-minimized crystal structure (Table I). This indicates that the wild-type enzyme–substrate complex remained stable during the 80-ps simulation run, and that the substrate binding did not significantly alter the energy minimum of the crystallographic structure. The distance between the

**TABLE II. Values of Stereochemical Parameters Detailing the Interaction of 2,5-DKG Substrate With NADPH Co-factor and Active-Site Residues<sup>†</sup>**

Enzyme–substrate complex	d1 (Å)	d2 (Å)	d3 (Å)	Degrees		Interaction enthalpy
				a1	a2	
DKGR A	2.5 (0.1)	2.0 (0.1)	2.0 (.1)	139 (11)	111 (16)	−35.0 (3.8)
(1–40 ps)	2.5 (0.1)	2.0 (0.1)	2.0 (.1)	134 (5)	123 (2)	−34.4 (2.8)
(41–80 ps)	2.5 (0.1)	2.0 (0.1)	2.0 (.1)	144 (4)	98 (2)	−35.7 (2.8)
Phe22Tyr	2.5 (0.1)	2.0 (0.1)	2.5 (0.1)	147 (4)	137 (5)	−36.6 (3.5)
(1–40 ps)	2.5 (0.1)	2.0 (0.1)	2.4 (0.1)	146 (5)	137 (5)	−36.8 (3.8)
(41–80 ps)	2.5 (0.1)	2.0 (0.1)	2.5 (0.1)	148 (5)	138 (5)	−36.4 (3.7)
Gln192Arg	2.5 (0.1)	2.9 (0.2)	1.8 (0.2)	120 (16)	153 (16)	−71.7 (4.4)
(1–40 ps)	2.5 (0.1)	3.0 (0.1)	1.9 (0.1)	111 (7)	148 (7)	−71.7 (4.4)
(41–80 ps)	2.5 (0.1)	2.8 (0.1)	1.8 (0.1)	128 (7)	158 (7)	−71.8 (4.4)
Phe22Tyr/Gln192Arg	2.6 (0.1)	2.8 (0.2)	1.9 (0.2)	123 (29)	137 (5)	−66.1 (4.5)
(1–40 ps)	2.6 (0.1)	2.7 (0.4)	1.9 (0.1)	134 (28)	136 (5)	−67.2 (4.6)
(41–80 ps)	2.6 (0.1)	3.0 (0.3)	1.9 (0.1)	111 (24)	138 (5)	−64.8 (4.2)

<sup>†</sup>Values in parentheses show the standard deviation. For definition of d1, d2, d3, a1, and a2, see Figure 3.

4-pro-*R*-hydrogen of the nicotinamide ring and the C5 carbonyl carbon of the substrate varied between 2.3 and 2.8 Å (with an average of 2.5 Å) over the course of molecular dynamics (Fig. 3). This is an essential feature for the first step of the reduction reaction because hydride ion ( $H^-$ ) transfer to the substrate requires this magnitude of cofactor–substrate proximity.<sup>10,16</sup> Subsequently, a proton ( $H^+$ ) transfer to the substrate oxyanion group would depend upon appropriate juxtaposition with the Tyr50  $O_{\eta}H$  group, the postulated proton donor in the active site.<sup>3,8,18–20</sup> During the 80-ps MD calculations, the substrate C5 OH group maintained an average distance of about 2.0 Å with the Tyr50  $O_{\eta}$  proton.

The general binding geometry of 2,5-DKG to wild-type DKGR A agrees well with the proposed “anion” binding site in the related human aldose reductase.<sup>14</sup> The sugar substrate, a pyranose ring with a “chair” conformation, binds toward the “A” face of the nicotinamide ring in the active site pocket. This causes the plane of the substrate pyranose ring to lie nearly parallel to the nicotinamide ring. The bound substrate displaces solvent groups 332 and 381 present in binding pocket of the X-ray crystal structure. The C4 OH essentially displaces sol 381, and the C5 keto group displaces sol 332 (Fig. 2A–D). The substrate makes interactions with the enzyme and co-factor primarily through the C4 and C5 groups. The C4 hydroxyl group hydrogen bonds with the  $N_{\epsilon}1$  atom of Trp 109 and the keto oxygen of the nicotinamide group of the NADPH co-factor (Table II). The C5 *keto* group of the substrate, which undergoes the reduction reaction, is hydrogen bonded to the  $O_{\eta}$  atom of Tyr50 (the proton donor group in the reaction) and the  $N_{\epsilon}2$  atom of His108. The C5 atom itself is positioned 2.6 Å from the 4-pro-*R* hydrogen of the reduced NADPH co-factor, the source of the hydride ion transferred during the reduction reaction.<sup>8</sup> The remaining interactions of the bound substrate involve van der Waals interactions of C6 with the Phe side chain at position 22; all other interactions are directly with solvent. These interactions yield a total of −32 kcal/mol of interaction enthalpy between the substrate and enzyme (Table II).

### Substrate Binding in Phe22Tyr DKGR A

A stereo view of the averaged molecular dynamics structures for the Phe22Tyr mutation of wild-type DKGR A, with bound 2,5-DKG substrate, is shown in Figure 2 (E and F). The side chain  $O_{\eta}$  group at position 22 is accommodated with almost no change in the enzyme–substrate complex. The introduced  $O_{\eta}$  group at this position is ideally juxtaposed to form a new hydrogen bond with the substrate C1-carboxylate group (Fig. 2E and F). This results in an overall interaction enthalpy of −36.6 kcal/mol, indicating that this single novel hydrogen bond is contributing approximately 4.0 kcal/mol of additional binding energy. Overall, the conformation of the Phe22Tyr mutant and its active site residues do not change significantly from the native structure as demonstrated by root mean square deviation values (Table I). As in the wild-type enzyme–substrate complex, a major contribution to the binding energy comes from the interaction of the C5-carbonyl group of the sugar with Tyr50 ( $O_{\eta}H$ ) and His108  $N_{\epsilon}H$ .

### Substrate Binding in Gln192Arg DKGR A

A stereo view of the averaged molecular dynamics structures for the Gln192Arg mutation of wild-type DKGR A, with bound 2,5-DKG substrate, is shown in Figure 2 (G and H). The active site of the Gln192Arg mutant enzyme is slightly distorted as compared to the wild-type, or Phe22Tyr, complex. This is also evident in the root mean square deviation of individual side chains lining the catalytic site of enzyme (Table I). The arginine side chain at position 192 forms a direct salt bridge with the substrate C1-carboxylate group. This electrostatic interaction results in a rotation of the substrate pyranose ring by about 12–13 degrees along an axis perpendicular to the nicotinamide ring of the co-factor (Fig. 2G and H). The distance between Tyr50  $O_{\eta}H$  and substrate C5-carbonyl oxygen increases from 2.0 to 2.9 Å. Thus, in response to the electrostatic interaction with the Arg side chain at position 192, the 2,5-DKG substrate appears to be pulled away somewhat from the Tyr50  $O_{\eta}H$  group. The distance between the substrate C5-carbonyl

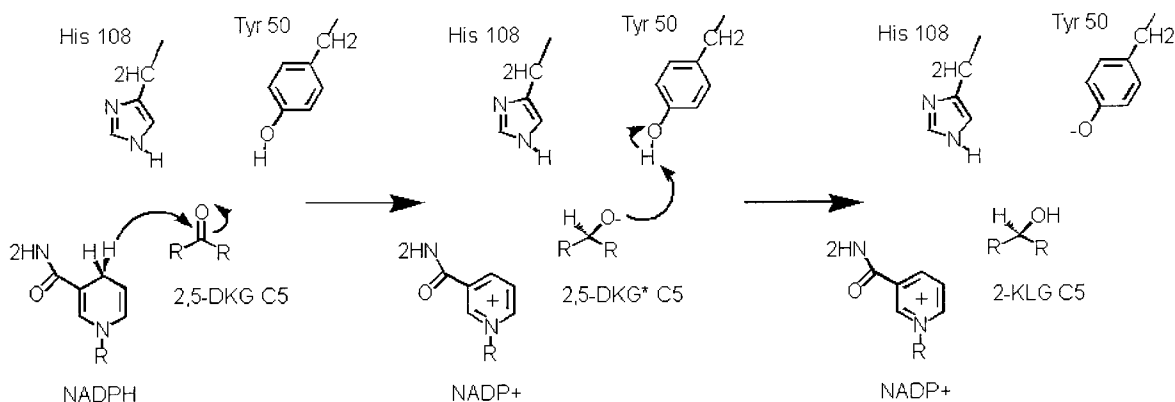


Fig. 4. Detail of the reaction mechanism for 2,5-DKGR based upon the aldo-keto reductases.<sup>14</sup> Tyr 50 O $\eta$ H group undergoes deprotonation during the reduction reaction, and is subsequently protonated by Lys74.

The His108 N $\epsilon$ H group hydrogen bonds with the substrate C5 keto group. It is postulated that this interaction preferentially positions the keto vs. the *gem*-diol form of substrate for reduction.

keto group and the His108 N $\epsilon$ H group remains essentially unchanged (Table II).

The major contribution to the interaction enthalpy between substrate and the Gln192Arg mutant arises from the electrostatic interaction between positively charged Arg192 side chain and negatively charged substrate C1-carboxyl group. The rest of the hydrogen bonding network in the Gln192Arg–2,5-DKG complex remains similar to the wild-type complex except for reduction in the interaction energy between Tyr50 O $\eta$ H and substrate C5-carbonyl group. As observed in the wild-type complex, the 4-hydroxyl group of the substrate and Trp109 N $\epsilon$ H form a hydrogen bond, which stabilizes the complex. The 2 and 3-hydroxyl groups of substrate, which face toward the outside of the sugar-binding cavity, interact with water molecules (not shown). The total interaction enthalpy between Gln192Arg and substrate amounts to  $-71$  kcal/mol, which is nearly double that of the wild-type complex.

#### Substrate Binding in Phe22Tyr/Gln192Arg DKGR A

A stereo view of the averaged molecular dynamics structures for the Phe22Tyr/Gln192Arg double mutant, with bound 2,5-DKG substrate, is shown in Figure 2 (I and J). The Tyr side chain at position 22 in the DKGR A point mutant hydrogen bonds with the substrate C1 carboxyl group (Fig. 2E and F). However, in the double mutant this side chain hydrogen bonds with the substrate C1 OH group (Fig. 2I and J). This alteration of hydrogen bonding pattern with the substrate is a result of the electrostatic interaction with the arginine side chain introduced at position 192. The Arg192 side chain participates in an electrostatic interaction with the substrate C1 carboxyl group, in a similar manner as the Arg192 point mutation (Fig. 2G and H). The hydrogen bonding distances to the key catalytic and co-factor atoms are similar to the Arg192 point mutation (Tables I and II), albeit with some slight distortion. This distortion is a consequence of the interaction of the mutant tyrosine residue at position 22.

## DISCUSSION

The general proposed mechanism of catalysis by aldo-keto reductases constitutes a two-step process as described for human aldose reductase.<sup>3,18,20</sup> The first step involves the transfer of a hydride ion ( $\text{H}^-$ ) from NADPH to the substrate C5-carbonyl carbon atom. It has been experimentally shown for DKGR A and other members of the aldo-keto reductase superfamily that transfer of the 4-*pro-R*-hydrogen from C4 of the nicotinamide ring carries out this step.<sup>8</sup> This is also supported by the crystal structure of DKGR A which shows that the nicotinamide ring binds deep in the active site of the enzyme with the 4-*pro-R*-hydrogen facing the opening of the substrate binding pocket.<sup>5</sup> This step of hydride transfer leaves an oxidized co-factor along with the tetrahedral intermediate form of substrate, which is  $\text{sp}^3$  hybridized at the C5-carbonyl carbon atom. Concomitant with this, a complete reduction reaction would also require the protonation of the substrate C5-oxyanion from a proton-donating functional group of the enzyme.

The crystal structure of human aldose reductase and other members of the aldo-keto reductase family reveal that there are two possible candidates for such a proton donor: Tyr50 (Tyr48 in human aldose reductase) and His108 (His110 in human aldose reductase).<sup>5,18</sup> Between these, Tyr50 is considered the more likely proton donor group mainly because it is involved in hydrogen bonding with Lys75, which is expected to lower its  $\text{pK}_a$  and facilitate proton donation.<sup>3,20</sup> Site-directed mutagenesis experiments have supported the proposed role of Tyr48 as the proton donor for human aldose reductase using glyceraldehyde as substrate.<sup>20,21</sup> Replacing Tyr48 in human aldose reductase with phenylalanine completely abolishes activity, whereas replacing His110 (corresponding to His108 in DKGR A) with alanine decreases  $k_{\text{cat}}/K_m$  for the enzyme by about 26,000 fold.<sup>21</sup> Recent kinetic studies with human aldose reductase also favor Tyr48 as the proton donor.<sup>22–24</sup> The overall reaction mechanism is detailed in Figure 4.<sup>14</sup> Alternatively, Schelegel et al.<sup>19</sup> have proposed

a “push-pull” mechanism for proton transfer in  $3\alpha$ -hydroxysteroid dehydrogenase, a member of aldo-keto reductase superfamily. According to this mechanism, His117 (equivalent to His108 in 2,5-DKGR A) facilitates proton donation and Lys84 (Lys 75 in 2,5-DKGR) facilitates proton removal from Tyr55 (Tyr50 in 2,5-DKGR) for the reduction and oxidation reactions, respectively. However, such a “push-pull” mechanism cannot be invoked for 2,5-DKGR, because the distance between His108 N $\epsilon$  and Tyr50 O $\eta$  is 4.5 Å (according to the crystal structure of 2,5-DKG), which is not conducive for proton donation.<sup>5</sup>

In this study, we have developed a model for the 2,5-DKG substrate in complex with the wild-type and mutant DKGR A enzymes. The 2,5-DKG substrate was modeled in the reaction-competent keto-form, although the *gem*-diol form is the predominant form in solution.<sup>11,12</sup> The interaction of the substrate C5-keto with the His108 N $\epsilon$ H and Tyr50 O $\eta$  groups suggests that juxtaposition of one, or both, of these groups facilitates binding of the keto-form of the substrate in solution. In particular, the interaction of the keto group with His108 may position the substrate C5 carbon for effective hydride transfer from the NADPH cofactor. This role for His108 is supported by the conserved H-bond interaction between this residue and the substrate C5 carbonyl (Table II). Hydrogen bonding of Tyr50 with the substrate C5 keto group appears to be more tenuous (Table II). The reaction intermediate, having tetrahedral geometry at the C5 carbon, would position the C5 oxyanion closer toward the Tyr50 group for proton donation. DKGR A and B exhibit several amino acid substitutions within the region of the active site, including positions 22 and 192. Substitutions at these positions in DKGR A, to the corresponding residues of DKGR B, results in the introduction of new hydrogen bonding and electrostatic interactions with the bound substrate. Together, these results suggest that the substrate is correctly positioned within the active site.

The Phe  $\rightarrow$  Tyr substitution at position 22 causes a 2.5-fold decrease in  $K_m$  for 2,5-DKG from 31.2 to 12.3  $\mu$ M, whereas the value of  $k_{cat}$  remains essentially unchanged (from 8.4 to 8.7  $\text{sec}^{-1}$ ).<sup>8</sup> The introduction of a Tyr residue at position 22 is accomplished without alteration of the substrate alignment in the binding pocket. The only significant change is the additional hydrogen bonding interaction with the substrate C1 carboxylate group. Because the alignment of the 5C keto group with the NADPH 4-*pro-R* hydrogen, and the Tyr50 O $\eta$  group is unaffected, this provides a rationale as to why the  $k_{cat}$  rate remains essentially unchanged with this mutation. The decrease in  $K_m$  is therefore attributed to the introduction of the additional hydrogen bonding interaction with the substrate C1 group.

The Gln  $\rightarrow$  Arg substitution at position 192 in DKGR A primarily affects the  $k_{cat}$  parameter toward the 2,5-DKG substrate, increasing its value approximately 2.5-fold, whereas  $K_m$  is relatively unaffected, or increases slightly.<sup>8</sup> The introduction of an Arg residue at this position results in a noticeable change in the orientation of the substrate within the binding pocket (Fig. 2G and H). This orientation

change primarily affects the substrate geometry with the Tyr50 O $\eta$  group, whereas the juxtapositions to the co-factor NADPH and His108 groups are unaffected (Table II). The observed increase in  $k_{cat}$  is thus attributed to a more favorable orientation with the Tyr50 O $\eta$  group for proton transfer to the tetrahedral intermediate. In this regard, interactions with the substrate C1 group may act as a lever arm to influence the orientation of the C5 keto group owing to the hydrogen bond between the C5 keto and the N $\epsilon$ 2 of His108. DKGR A and B are both acidic proteins, containing approximately 16% glutamate and aspartate residues.<sup>1,25</sup> However, the active site pocket exhibits a positive electrostatic characteristic ranging over the region described by residues 75, 108, and 109 (Fig. 2A–D). The positive nature of the active site pocket, juxtaposed against the background of an acidic protein, may help steer the acidic substrate toward the active site. The modeling results suggest that the Gln192Arg mutation, in addition to introducing a direct salt bridge between the enzyme and substrate, increases the positive electrostatic characteristic of the substrate binding pocket (Fig. 2G and H). Thus, this mutation may also affect the steering of substrate to the active site.

The effects of the individual point mutations at positions 22 and 192 upon the kinetic constants of DKGR A are reportedly nonadditive, with the double mutant exhibiting similar kinetic constants to the wild-type DKGR A enzyme.<sup>8</sup> The interaction of the Tyr side chain at position 22 with the substrate C1 carboxyl group, observed in the point mutant, is disrupted with the introduction of the Arg side chain at position 192.

Thus, the reduction in  $K_m$  seen in the Tyr 22 point mutant is not observed in the double mutant. The interaction of substrate with the Arg192 side chain in the double mutant appears to be very similar to that observed in the Arg192 point mutant. However, the 2.5-fold increase in  $k_{cat}$  displayed by the Arg192 point mutant is not seen in the double mutant. Thus, the tyrosine side chain at position 22 may interfere with alignment of the substrate for efficient hydride transfer from co-factor, or proton transfer from Tyr50. The residues at positions 22 and 192 in DKGR B are, however, tyrosine and arginine, respectively, and DKGR B exhibits higher  $k_{cat}$  and lower  $K_m$  values in comparison to DKGR A. Thus, although the combination of these two residues in the active site of DKGR A does not lead to improved catalysis toward 2,5-DKG, in the active site of DKGR B they may well contribute to the observed enhanced catalytic constants. Therefore, knowledge of the active site geometry of DKGR B appears essential to understand fully the role of these residues in enhancing catalysis toward 2,5-DKG.

The results of this modeling study indicate that although the active site pocket of DKGR A can perform the stereo-specific reduction of 2,5-DKG to 2-KLG, the active site may not be optimized for this substrate. Several hydroxyl groups of the bound substrate have solvent as hydrogen-bonding partners. The Tyr mutation at position 22 suggests that mutations that introduce appropriate hydrogen-bonding partners within the active site may

contribute to lower  $K_m$  values. Additionally, the orientation of the 2,5-DKG in the wild-type enzyme may not be oriented ideally for resolution of the oxyanion tetrahedral intermediate via proton donation by Tyr50. The Arg mutation at position 192 suggests that mutations can be introduced to improve alignment of the substrate for proton transfer by Tyr50. Other areas for further investigation into improving 2,5-DKG catalysis might include mutations to increase the positive electrostatic nature of the binding site (to improve steering of substrate to the active site) as well as mutations to decrease the size of the active site pocket (and increase van der Waals contacts with the substrate).

### ACKNOWLEDGMENTS

We thank Drs. Tim Logan and Michael Chapman for reading the manuscript and for helpful discussions. Technical support from Molecular Simulations Inc., San Diego is acknowledged. D.P. and S.A. were supported by NIH grants GM08339, R01AG11525, and R01GM50733.

### REFERENCES

- Anderson S, Marks CB, Lazarus R, Miller J, Stafford K, Seymour J, Light D, Rastetter W, Estell D. Production of 2-keto-L-gulonate, and intermediate in L-ascorbate synthesis, by a genetically modified *Erwinia herbicola*. *Science* 1985;230:144–149.
- Sonoyama T, Tani H, Matsuda K, Kageyama B, Tanimoto M, Kobayashi K, Yagi S, Kyotani H, Mitsushima K. Production of 2-keto-L-gulonic acid from D-glucose by two-stage fermentation. *Appl Environ Microbiol* 1982;43:1064–1069.
- Jez JM, Bennett MJ, Schlegel BP, Lewis M, Penning TM. Comparative anatomy of the aldo-keto reductase superfamily. *Biochem J* 1997;326:625–636.
- Reichstein T, Grussner A. Eine ergiebige synthese der L-ascorbinsäure (C-Vitamin). *Helv Chim Acta* 1934;17:311–328.
- Khurana S, Powers DB, Anderson S, Blaber M. Crystal structure of 2,5-diketo-D-gluconic acid reductase A complexed with NADPH at 2.1 Å resolution. *Proc Natl Acad Sci USA* 1998;95:6768–6773.
- Hoog SS, Pawlowski JE, Alzari PM, Penning TM, Lewis M. Three-dimensional structure of rat liver 3 $\alpha$ -hydroxysteroid/dihydrodiol dehydrogenase: a member of the aldo-keto reductase superfamily. *Proc Natl Acad Sci USA* 1994;91:2517–2521.
- Wilson DK, Nakano T, Petrash JM, Quioco FA. 1.7 Å structure of FR-1, a fibroblast growth factor induced member of the aldo-keto reductase family, complexed with coenzyme and inhibitor. *Biochemistry* 1995;34:14323–14330.
- Powers D. Structure/function studies of 2,5-diketo-D-gluconic acid reductases. Piscataway, NJ: University of Medicine and Dentistry of New Jersey; 1996. 163 p.
- Dauber-Osguthorpe P, Roberts VA, Osguthorpe DJ, Wolff J, Genest M, Hagler AT. Structure and energetics of ligand binding to proteins: E. coli dihydrofolate reductase-trimethoprim, a drug receptor system. *Proteins: Structure function and genetics*. 1988;4:31–47.
- Daffron TR, Badcoe IG, Sessions RB, Hawrani ASE, Holbrook JJ. Correlation of the enzyme activities of *Bacillus stearothermophilus* lactate dehydrogenase on three substrates with the results of molecular dynamics/energy minimization conformational search. *Proteins* 1997;29:228–239.
- Andrews GC, Bacon BE, Bordner J, Hennessee GLA. The Structure of D-threo-2,5-hexodiulosonic acid and derivatives in solution. *Carbohydr Res* 1979;77:25–36.
- Crawford TC, Crawford SA. Synthesis of L-ascorbic acid. *Adv Carbohydr Chem Biochem* 1980;37:79–155.
- Miller JV, Estell DA, Lazarus RA. Purification and characterization of 2,5-diketo-D-gluconic acid reductase from *Corynebacterium* Sp. *J Biol Chem* 1987;262(July 5):9016–9020.
- Harrison DH, Bohren KM, Ringe D, Petsko GA, Gabbay KH. An anion binding site in human aldose reductase: mechanistic implications for the binding of citrate, cacodylate, and glucose-6-Phosphate. *Biochemistry* 1994;33:2011–2020.
- Allen MP, Tildesley DJ. Computer simulation of liquids. In: Press C, editor. Oxford Science Publications; 1987.
- Winter HLD, Itzstein MV. Aldose reductase as a target for drug design: molecular modeling calculations on the binding of acyclic sugar substrates to the enzyme. *Biochemistry* 1995;34:8299–8308.
- Gilson MK, Honig BH. Energetics of charge-charge interactions in proteins. *Proteins* 1988;3(1):32–52.
- Wilson DK, Bohren KM, Gabbay KH, Quioco FA. An unlikely sugar substrate site in the 1.65 Å structure of the human aldose reductase holoenzyme implicated in diabetic complications. *Science* 1992;257:81–84.
- Schlegel BP, Jez JM, Penning TM. Mutagenesis of 3-alpha-hydroxysteroid dehydrogenase reveals a “push-pull” mechanism for the proton transfer in aldo-keto reductases. *Biochemistry* 1998;37:3538–3548.
- Tarle I, Borhani DW, Wilson DK, Quioco FA, Petrash JM. Probing the active site of human aldose reductase. Site directed mutagenesis of Asp 43, Tyr 48, and His 110. *J Biol Chem* 1993;268:25687–25693.
- Bohren KM, Grimshaw CE, Lai C-J, Harrison DH, Ringe D, Petsko GA, Gabbay KH. Tyrosine-48 is the proton donor and histidine-110 directs substrate stereochemical selectivity in the reduction reaction of human aldose reductase: enzyme kinetics and crystal structure of the Y48H mutant of enzyme. *Biochemistry* 1994;33:2021–2032.
- Grimshaw CE, Bohren KM, Lai CJ, Gabbay KH. Human aldose reductase: pK of tyrosine 48 reveals the preferred ionization state for catalysis and inhibition. *Biochemistry* 1995;34(44):14374–14384.
- Grimshaw CE, Bohren KM, Lai CJ, Gabbay KH. Human aldose reductase: subtle effects revealed by rapid kinetic studies of the C298A mutant enzyme. *Biochemistry* 1995;34(44):14366–14373.
- Grimshaw CE, Bohren KM, Lai CJ, Gabbay KH. Human aldose reductase: rate constants for a mechanism including interconversion of ternary complexes by recombinant wild-type enzyme. *Biochemistry* 1995;34(44):14356–14365.
- Grindley JF, Payton MA, van de Pol H, Hardy KG. Conversion of glucose to 2-keto-L-gulonate, an intermediate in L-ascorbate synthesis, by a recombinant strain of *Erwinia citreus*. *Appl Environ Microbiol* 1988;54(7):1770–1775.